

Original Paper

# Antibacterial Activity of Silver Nanoparticles Prepared from *Camellia Sinensis* Extracts in Multi-Drug Resistant *Staphylococcus Aureus*

Hawazen Salih<sup>a</sup> Rami Altameemi<sup>a</sup> Ahmed AL-Azawi<sup>a</sup>

<sup>a</sup>Genetic Engineering and Biotechnology Institute for post graduate studies, University of Baghdad, Baghdad, Iraq.

## Key Words

Antibacterial activity • Anti-biofilm activity • *Camellia sinensis* • Nanoparticles • *Staphylococcus aureus*.

## Abstract

**Background/Aims:** The nano-method has been used as a technique for creating novel, non-traditional antimicrobial agents. This effective method for treating infectious diseases has many advantages over conventional antibiotics, including increased efficacy against species that have developed drug resistance, and the ability to circumvent the development of resistance that disrupts a number of biological pathways. As a result, the objective of this study was to synthesize and characterize silver nanoparticles using phenolic compounds obtained from *Camellia sinensis*. The nanoparticles were then used as antibacterial agents on the multidrug resistant *Staphylococcus aureus*, as well as, biofilm formation mechanism were also investigated.

**Methods:** Ten isolates of *Staphylococcus aureus* were acquired from the labs of the University of Baghdad's Genetic Engineering and Biotechnology Institute. The VITEK-2 system was used to confirm the diagnosis. Aqueous and methanolic extracts of *Camellia sinensis* leaves were used to create silver nanoparticles and obtain CAgNPs, which were then characterized using Atomic Fluorescence Microscopy (AFM), X-ray diffractometer (XRD), and Zeta potential analyzers. The extracts were put through a series of assays, including High-performance liquid chromatography (HPLC), antibacterial activity assessments, and the microtiter plate method to determine the lowest inhibitory concentration (MIC) and antibiofilm formation. **Results:** Both aqueous and methanolic extracts containing silver nanoparticles included spherical nanoparticles that may be single or combined. The HPLC results showed the presence of two phenolic compounds (gallic acid and caffeine) by comparing their retention durations to those of the reference compounds. The results of the antibacterial activity of (CAgNPs) showed that the methanolic (CAgNPs) extract was more effective than the aqueous (CAgNPs) extract, producing inhibitory zones of  $15.67 \pm 0.58$  and  $20.33 \pm 0.58$  mm, at 375 and 750 ppm

respectively, when compared to the aqueous (CAGNPs) extract, which produced inhibitory zones of  $12.33 \pm 0.58$  and  $15.67 \pm 0.58$  mm, respectively. The MIC result also showed that the CAGNPs methanolic extract was more effective than the CAGNPs aqueous extract. The MIC of the CAGNPs methanolic extract on *S. aureus* isolates were 11.718 and 23.43  $\mu\text{g/ml}$ , while the MIC of the CAGNPs aqueous extract on all *S. aureus* isolates were 46.87  $\mu\text{g/ml}$  except isolate No. 3 and 6 which was 11.718 and 93.75  $\mu\text{g/ml}$  respectively. Additionally, The anti-biofilm in *S. aureus* was increased when CAGNPs methanolic extract were used compared with the CAGNPs aqueous extract, the CAGNPs methanolic extract inhibited 80%, 90% and 100% of the biofilm formation of *S. aureus* in 23.43, 46.87 and 93.75  $\mu\text{g/ml}$  respectively, while the anti-biofilm activity of the CAGNPs aqueous extract on *S. aureus* isolates was 80% and 100% of the biofilm formation in 46.87 and 93.75  $\mu\text{g/ml}$  respectively. **Conclusion:** The methanolic and aqueous leaves extracts from *Camellia sinensis* are a successful method for producing CAGNPs. The synthesized CAGNPs also have significant antibacterial activity against *S. aureus*, depending on the concentrations, and inhibit *S. aureus* biofilm formation.

© 2024 The Author(s). Published by  
Cell Physiol Biochem Press GmbH&Co. KG

## Introduction

*Staphylococcus aureus* is a widespread, virulent pathogen that is linked to a wide range of infections. These infections can range from minor local infections of the skin and soft tissues to serious systemic infections like sepsis and toxic shock syndrome, which can be fatal. Since the 1960s, patients in hospitals, nursing homes, and other healthcare institutions have increasingly been affected by these bacteria, which often reside as a commensal in the nose and/or throat of 20% to 70% of adults and are typically resistant to numerous antibiotics [1]. A critical global problem is the development of antibiotic and antifungal treatment resistance in harmful bacteria and fungus species [2]. The ineffectiveness of the antimicrobial drugs is mostly due to these microorganisms' formation of biofilms [3]. These harmful microbes can withstand 1,000 doses of conventional antibacterial medications when they are in the form of biofilms [4]. Resistance-building capacity of bacteria outperforms the development of new, powerful antibiotics. Additionally, there are a number of important drawbacks to current antimicrobial therapy, including their lack of diversity, antagonistic interactions, and the consequences of incomplete antibiotic use, which can result in the development of microbial resistance. Unfortunately, the rate of multi-resistant bacteria evolution has outpaced the rate of new antibiotic discovery; consequently, the development of innovative and effective antimicrobial therapies is crucial [5]. Therefore, it is now more crucial than ever to create a novel, potent treatment strategy in order to eliminate and manage resistant bacteria. Nanomaterials having antibacterial characteristics can be used as a solution to this widespread issue. In order to combat the issue of antibiotic resistance, with the development of nanotechnology, plant extracts are now being used to create nanoscale materials. Nanotechnology is gaining prominence in the present day because to the biological modeling of metals in nanoparticles (NPs), and nanoparticle manufacturing, particularly of silver nanoparticles, has gained prominence due to its characteristics, biocompatibility, and uses. At the moment, nanoparticle synthesis procedures are geared towards the development of low-cost, simple, non-toxic, and environmentally acceptable approaches. Thus, the use of plants in the synthesis of silver nanoparticles has generated a great deal of interest because their secondary metabolites contain chemically active components that can function as capping and reducing agents, speeding up the reduction and stabilization of NPs [6].

## Materials and Methods

### *Bacterial Isolates*

Ten isolates of *P. aeruginosa* were obtained from the genetic engineering and biotechnology institute/ University of Baghdad. These isolates were previously identified by molecular and chemical testing after

being gathered from many hospitals in Baghdad. The isolates were incubated at 42°C for 18–24 hours on cetrinide agar, and use the VITEK-2 in order to confirm the diagnosis.

### *Antibiotic susceptibility test*

The World Health Organization (WHO) [7] suggests using the Clinical Laboratory Standard Institute (CLSI) modified Kirby-Bauer disc diffusion method to encourage reproducibility and comparison of results between laboratories. Ten antibiotics including Azithromycin, Chloramphenicol, Rifampin, Methicillin, Tetracycline, Vancomycin, Gentamicin, Erythromycin, Ciprofloxacin, Cefoxitin have been evaluated using this approach for susceptibility testing. This well-known approach involves inoculating a standard inoculum of the test organism onto a 150 mm diameter Muller Hinton Agar (MHA) plate, which equates (1.5 x 10<sup>8</sup> colony forming units/ml). The bacterium Isolates is then covered with antibiotic discs (about 6 mm in diameter; commercially available). Agar plates are often incubated at 37 °C overnight to allow antimicrobial chemicals to diffuse into the agar and suppress bacterial growth. Using a sliding caliper or a ruler, the inhibition zone is manually measured in millimeters, and the diameter of the inhibition zone yields qualitative findings for the susceptible, intermediate, or resistant bacteria according to CLSI [8].

### *Assessment of biofilm formation*

The colorimetric microtiter plate technique, as previously published by Patel et al [9], was used to quantitatively evaluate the production of biofilms with certain changes. *S. aureus* overnight culture was brought up to a 0.5 McFarland level of turbidity. Following a 1:100 dilution in 200 µl of sterile, flat-bottomed polystyrene micro-plates with a 1% glucose concentration, the suspensions were put there. After 24 hours of incubation at 37 °C, the wells were gently rinsed three times with sterile phosphate buffered saline (PBS, pH 7.3). The plate was air-dried after the adherent biofilms were fixed with 99% methanol for 15 min. Biofilms were stained for 5 minutes at room temperature with 200 µl of crystal violet 0.1%, then washed with water and given time to dry. By treating each well with 200 µl of 95% ethanol for 30 minutes, biofilm in each well was removed. A microtiter plate reader (ELISA) was used to measure the optical density (OD) at 630 nm. Three separate replications of each experiment were carried out in triplicate. In addition, a cut-off value (ODc) was established. It is defined as three standard deviations (SD) above the mean OD of the negative control:  $ODc = \text{average OD of negative control} + (3 \times SD \text{ of negative control})$ . The isolates were classified into the four following categories based upon the OD: non-biofilm producer ( $OD < ODc$ ); weak-biofilm producer ( $ODc < OD < 2 \times ODc$ ); moderate-biofilm producer ( $2 \times ODc < OD < 4 \times ODc$ ); strong-biofilm producer ( $4 \times ODc < OD$ ) [10].

### *Collection of Camellia sinensis L*

The *Camellia sinensis* leaves were gathered from Baghdad markets, and verified their authenticity by a botanical taxonomist at the College of Science's, Biology Department of the University of Baghdad. The leaves were thoroughly washed, air dried, and ground. First, the fat from 400 grams of powdered *Camellia sinensis* leaves was removed by macerating with two liters of petroleum ether solvent. Two batches of the residue were created, air-dried, and collected. To create aqueous and methanolic extracts, every batch of the defatted plant leaves was extracted individually using methanol and water. 200 g of each powdered plant material was dissolved in 1 liters (L) of sterile distilled de-ionized water and 1 liters (L) of methanol alcohol and placed in two separate extraction bottles. The mixtures were left to stand for 48 to 72 hours at room temperature, and with occasional daily stirring to ensure homogeneous mixing and extraction. After filtering using Whatman No. 1 filter paper, the extract was dried under reduced pressure at 40 °C by Rotary evaporator, to get a sticky residue after heating it in an oven at 37°C and then retaining it at 4°C for conduct studies [11].

### *Synthesis green silver nanoparticles using Camellia sinensis extracts*

By dissolving 1.69 g of AgNO<sub>3</sub> in 1 L of deionized water (DIW), a solution of AgNO<sub>3</sub> was created, and stored in an amber bottle in a cool and dry place. Aqueous and methanolic extracts of *Camellia sinensis* were used to create green silver nanoparticles. Five ml of each extract was sprayed dropwise into 95 ml of a 10 mM silver nitrate AgNO<sub>3</sub> solution at 0.2 ml/min as the rate while utilizing an ultrasonic generator with a 100 W power output and a 42 kHz frequency. The solutions were sonicated for 20 minutes, agitated at 800 rpm at 25°C for 30 minutes, and then held there for 48 hours. The reaction mixture was cleaned after 24

hours by centrifuging it for 10 minutes at 10,000 rpm to get a clear supernatant. For *Camellia sinensis* silver nanoparticles (CAGNPs), over the course of five days, the solutions' dark green tint became yellow. This color shift denotes the development of silver nanoparticles (Ag-NPs). The final colloid samples were kept at 4°C in bottles that were dark [12].

### *Atomic force microscopy*

Under typical air circumstances, the surface morphology of the nanoparticles was seen using the Atomic Force Microscope Contact mode. Using an AA3000 scanning probe microscope, AFM examination was carried out. After being sonicated with distilled water, a little drop of each kind of nanoparticle sample was placed on a glass slide (1x1cm) and left to dry. The slide was then placed on the AFM sample stage, and analysis was performed as per usual protocol [13].

### *X-ray diffractometer*

X-Ray Diffraction was used to analyze structural characterization in order to learn more about surface morphology, crystal structure, and particle size. The diffractometer recorded in the range of  $20 \leq 2\theta \leq 90$  angles and uses Cu-  $K\alpha$  as an anode, at wavelength = 0.154060 nm. The scan step for  $2\theta$  was 0.0170°. For XRD examination, the filtrate drier nanoparticles were spread out on a glass grid comprising silicon substrate [14]. The XRD pattern result was interpreted using the Joint Committee on Powder Diffraction Standards' standard reference (JCPDS card number 04-0783) for the characterization of Ag-NPs [15]. The Debye-Scherrer equation may be used to determine the average crystallite size.

$$D_{hkl} = K \times \lambda / \beta_{hkl} \cos \theta_{hkl}$$

Where  $D_{hkl}$  is the crystallite size,  $k$  is a constant (0.9),  $\lambda$  is the wavelength of X-ray,  $\beta_{hkl}$  is the full width at half maximum and  $\theta_{hkl}$  is the Bragg angle [16].

### *UV-Visible Absorption Spectroscopy*

UV-Visible spectroscopy proved that the silver ions in the colloidal solution had been reduced. With pure water used as a reference, a tiny aliquot of Ag NPs was placed in a quartz cuvette and monitored for wavelength scanning between 200 and 800 nm. After adding green tea extract to an AgNO<sub>3</sub> solution, the UV-Vis absorption spectra of the sample was measured using a Perkin Elmer Spectrophotometer at various times of 5, 10, 15, and 20 minutes [17].

### *Zeta potential analyzer*

Zeta potential analysis, which permits flow from -160 mV to +160 mV, was used to assess the stability of the synthesized nanoparticles, and the data were shown in a graph [18].

### *High-Performance Liquid Chromatography (HPLC)*

According to Mizzi et al. [19], aqueous and methanolic (CAGNPs) extract preparations were distinguished by (HPLC).

### *Examine the CAGNPs extracts as antibacterial agents*

*Method of disc diffusion.* The disc diffusion technique for the antibacterial activity described by Razmavar et al [20], was used to determine if the (CAGNPs) methanolic and aqueous extracts had the antibacterial activity. *Staphylococcus aureus* were uniformly spread on Muller Hinton agar plates (0.5 McFarland). The plates were dried for 15 minutes before to the sensitivity test. The methanolic and aqueous extracts of the CAGNPs were employed at concentrations of 375 and 750 ppm. Then, 6 mm diameter sterile blank discs were impregnated with 20  $\mu$ l of each dilution, negative controls were used DMSO discs and distilled water. The dishes were incubated at 37 °C for 18 to 24 hours. By measuring the inhibitory zone surrounding the discs after the incubation, the antibacterial activity was assessed; each test was run three times.

*Measurement the MIC of the (CAGNPs) extracts.* Using the broth microdilution method, a 96-well microtiter plate was used to determine the (MIC) of the (CAGNPs) extracts. The concentration of the CAGNPs extract solution was 375 g/ml in broth, and subsequent two-fold dilutions of the extract were made on the plate to achieve concentrations of 2.92, 5.85, 11.718, 23.43, 46.87, 93.75, 187.5, and 375  $\mu$ g/ml. 200  $\mu$ l of the extracted methanolic and aqueous CAGNPs were introduced to the first wells of row A. Rows B through

H in columns each held 100 µl of broth. Twofold serial dilutions were systematically carried out down the columns (rows A–H). Row A starting concentrations were extracted using 100 µl, then moved to row B with 100 µl of properly mixed broth. This process continued until row H when the final 100 µl was discarded. As a result, all of the test wells' total extract volumes have increased to 100 µl, with the exception of the column, which got 200 µl of the sterility control soup. 100 µl of the  $1 \times 10^6$  CFU/ml bacterial inoculum were added to each well, except the negative control. The incubation period for microtiter plates was 18 to 20 hours at 37 °C. 20 µl of resazurin dye was added to each well and allowed to incubate for 30 minutes before examining the results to determine whether any color changes had taken place. Broth micro dilutions were used to visually determine the lowest concentrations of extracts at which the resazurin broth test revealed no color shift from blue to pink [21].

#### *Examine the anti-biofilm activity of the CAgNPs extracts*

A 96-well microtiter plate was used to test the anti-biofilm activity of the methanolic and aqueous extracts of CAgNPs. The concentration of the CAgNPs extract solution was 375 g/ml in broth, and subsequent two-fold dilutions of the extract were made on the plate to achieve concentrations of (375, 187.5, 93.75, 46.87, 23, 43, 11.718, 5.85, and 2.92) µg/ml. The first wells in row A received 200 µl of each sample of the methanolic and aqueous extracts of (CAgNPs) and broth. Only 100 µl of the broth were contained in Columns B through H. Double serial dilutions using a micropipette were carried out gradually down the columns (beginning with rows A–H). After correctly mixing 100 µl of the 100 µl broth and removing 100 µl from the starting concentrations in row A, the final 100 l were eliminated after repeating the procedure up to row H. 106 CFU/ml bacterial inoculum were added to each well, except the negative control. The same procedure as mentioned in paragraph (*Assessment of biofilm development*) was used.

#### *Statistical Analysis*

Least Significant Difference (LSD)-Test was used to significantly compare between means at  $P \leq 0.05$  after the data obtained for various parameters were submitted to ANOVA using the Statistical Analysis System- SAS programmed (SAS, 2012) in accordance with Completely Randomized Design-CRD with three replicates.

## Results and Discussion

### Antibiotic susceptibility Test

The disc diffusion method using CLSI 8, criteria was used to evaluate the antibiotic susceptibility of *S. aureus* isolates. This test was conducted on ten antibiotics: (Azithromycin, Chloramphenicol, Rifampin, Methicillin, Tetracycline, Vancomycin, Gentamicin, Erythromycin, Ciprofloxacin, and Cefoxitin). The findings showed that *S. aureus* isolates frequently exhibit significant levels of resistance to the antibiotics utilized in this investigation (Table 1). Four isolates of *S. aureus* were multi-drug resistant with a percentage of (80-100%), according to the anti-biogram of the examined isolates, whereas six isolates had a resistance range of (40-70). This skill is either naturally occurring or acquired by genetic material mutations or horizontal gene transfer [22]. The excessive antibiotic dosing has resulted in the building of antibiotic resistance and cross-resistance across antibiotics, as well as the formation of multi-drug resistant (MDR) forms of *S. aureus* [23].

To create fresh and cutting-edge antimicrobial treatments is critical given the rise of resistance isolates. In order to find better options to combat microbial populations that are multidrug-resistant, researchers are searching for fresh leads. Due to their extensive usage as treatments for a variety of infectious diseases and the abundance of bioactive substances they contain, plants have long been considered one of the possible sources of novel drugs [24].

Some of the findings of previous local and international investigations were thought to be fairly compatible with the current study. AbdulRazzaq [25] and his team of researchers found that *S. aureus* isolated from a number of clinical models from Baghdad hospitals was resistant to 61.4% of Azithromycin, 24% of Gentamicin, 30% of Levofloxacin, 52.8%

**Table 1.** Antibiotic susceptibility least of *S. aureus* isolates. S: *S.aureus*, (ATH): Azithromycin, (C): Chloramphenicol, (RP): Rifampin, (ME): Methicillin, (TE): Tetracycline, (VA):Vancomycin, (CN): Gentamicin, (E): Erythromycin, (CIP): Ciprofloxacin, (FOX): Cefoxitin

Antibiotic Isolate											Percentage of Resistance
	ATH	C	RP	ME	TE	VA	CN	E	CIP	FOX	
S1	S	R	S	R	R	S	R	R	R	R	70%
S2	R	R	S	R	R	S	R	R	S	R	70%
S3	S	S	R	S	R	R	S	R	S	R	50%
S4	R	R	R	R	R	R	S	R	S	R	80%
S5	R	S	R	S	R	S	R	I	S	R	50%
S6	R	R	R	R	R	R	R	R	R	R	100%
S7	R	S	R	S	R	S	S	R	R	R	60%
S8	S	R	S	R	S	S	S	I	R	R	40%
S9	R	R	R	S	R	R	S	R	R	R	80%
S10	R	R	S	R	R	R	R	R	S	R	80%

of Tetracycline, and 14.2% of Vancomycin. In a different study, Jabur and Kandala findings [26] on the susceptibility of *S. aureus* isolates (isolated from Post-Surgical Operation Inflammation) to different antimicrobial agents showed that all 68 isolates were totally resistant to cefotaxime and also displayed resistance to Ciprofloxacin, Trimethoprim, Vancomycin, and Gentamycin. The current study's findings were remarkably similar to those of the Al-Nuaimi et al [27]. study, which found that *S. aureus* isolates were 100% susceptible to ciprofloxacin and imipenem but 75% resistant to cefixime, 50% resistant to trimethoprim-sulfamethoxazole, and 25% susceptible to amikacin.

#### *Detection of the biofilm formation*

The Microtiter plate technique is utilized to detect the quantitative production of biofilms, and an ELISA reader was used to calculate the absorbance at 630 nm. The findings demonstrated that all isolates formed 100% robust biofilms.

In water systems, on a range of commonly present biotic surfaces in such systems, as well as in naturally occurring aquatic environments, bacteria can form biofilms. Biofilm production is one of the typical techniques bacteria adapt to survive under difficult environmental circumstances [28]. The ability of bacteria to form biofilms makes it easier for them to connect to host cells [29]. Because it provides a quick, easy, and accurate technique to measure the contact cell attachment and biofilm development of various bacterial strains, the microtiter plate has been the most popular and was thought of as a standard test for the detection of biofilm formation [30].

### Nanoparticle biosynthesis and characterization

Methanolic and aqueous extracts of *Camellia sinensis* were used to make the silver nanoparticles. Compared to other bioreductants, the production of metallic nanoparticles utilizing plant extracts is easier and more successful [31]. It is well known that phytochemicals cap the Ag<sup>+</sup> to produce these incredibly stable nanoparticles in addition to converting Ag<sup>+</sup> into Ag<sup>0</sup> [32].

This study followed the formation of silver nanoparticles using color change and UV spectroscopy absorption. The hues of the green silver nanoparticle solutions for *Camellia sinensis* silver nanoparticles (CAGNPs) shifted from dark green to light brownish green with the addition of *Camellia sinensis* methanolic and aqueous extracts, respectively, to silver nitrate solution. After 24 hours, the color started to shift, and after 48 hours, it transformed into the final shade that was indicated before. The presence of active molecules suggests that silver nanoparticles (AgNPs) were created by reducing silver metal ions Ag<sup>+</sup> into silver nanoparticles Ag<sup>0</sup> in the methanolic and aqueous extracts of *Camellia sinensis*.

Different metabolites found in plants, such as phenols, terpenoids, alkaloids, flavonoids, proteins, and carbohydrates, are essential for the stabilisation and conversion of metallic silver into Ag-NPs [33]. By lengthening the incubation period, it is possible to further accelerate the reduction rate and the production of nanoparticles, which causes the color's intensity to rise as the reaction time increases [34].

The shift in color is attributed to the activation of metal nanoparticles' surface plasmon resonance (SPR). A lot depends on the geometry of the nanoparticles for the optical properties of silver nanoparticles, which are fascinating and strongly connected to localized surface plasmon resonance [35]. This result is consistent with observations made by Saliem et al [34]. and Shareef et al [36]., who noted that color change may occur when silver ions are converted into silver nanoparticles following exposure to plant extracts. Ag-NP characterization is therefore essential for evaluating the functional attributes of the synthesized particles.

### Atomic force microscopy (AFM)

According to AFM analysis, the average particle size for the methanolic and aqueous extracts of CAGNPs was 84.76 nm and 108.3 nm, respectively, and were spherical in form, either individually or in aggregates (Fig. 1 and 2).

### X-ray diffractometer

An effective instrument for crystalline material characterization is the X-ray diffractometer (XRD), provides information on the phases of crystals, preferred orientations, and other structural traits including strain, crystallinity, average grain size, and crystal defects [37].

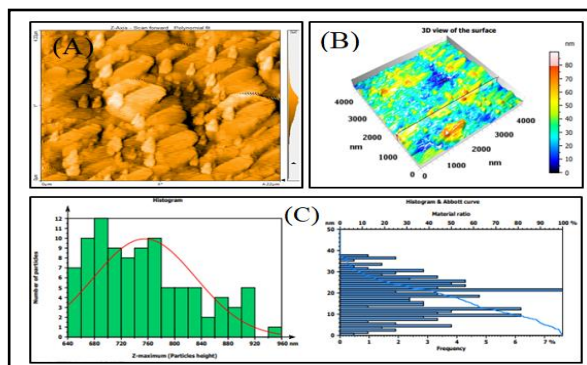


**Fig. 1.** AFM analysis of CAGNPs methanolic extract (A): 2-D of CAGNPs methanolic extract, (B): 3-D of CAGNPs methanolic extract, (C): Size distribution of CAGNPs methanolic extract shown in AFM graphic.

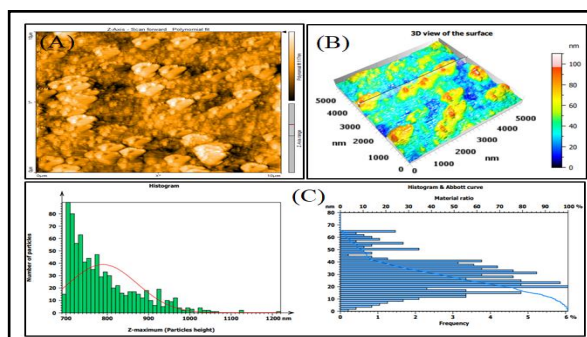


**Fig. 2.** AFM analysis of CAGNPs aqueous extract (A): 2-D of CAGNPs aqueous extract, (B): 3-D of CAGNPs aqueous extract, (C): Size distribution of CAGNPs aqueous extract shown in AFM graphic.

The green synthesis of AgNPs was further supported by X-ray diffraction (XRD). (Fig. 3) recorded obvious diffraction peaks at  $2\theta$  values 38.175, 44.325, 64.543, and 77.472 for CAgNPs methanolic extract which were corresponded to 111, 200, 220 and 311 planes of silver, while (Fig. 4) showed diffraction peaks at  $2\theta$  values 38.229, 44.349, 64.580, and 77.464 for CAgNPs aqueous extract corresponded to 111, 200, 220 and 311 planes of silver. The XRD pattern demonstrated the crystalline nature of the AgNPs created by the reduction of Ag<sup>+</sup> ions using *Camellia sinensis* extracts. Unassigned peaks were seen, which may have been caused by the bio-organic phase or by the presence of metalloproteins on the surface of the silver nanoparticles. Alternatively, it may have been caused by the plant extract's lower concentration of biomolecules that function as stabilizing agents, such as enzymes or proteins.

According to calculations using the Debye-Scherrer equation, the average crystallite sizes for the methanolic and aqueous extracts of CAgNPs are determined to be 61.24 and 99.66 nm, respectively. This result is consistent with the research of Ssekatawa et al [38]. Silver nanoparticles were produced by using an aqueous extract of *Camellia sinensis* bark, and they displayed distinct peaks of cubic phases at 38.0, 44.3, 64.5, and 77.4. The synthesis of silver nanoparticles by Rakaa and Obaid [39] using bark from thyme leaves as a starting material has resulted in clear cubic peak appearances at  $2\theta$ , which correspond to crystallographic planes 111, 200, 220, and 311. The peaks at 38.45°, 44.39°, 64.57°, and 77.54°, respectively. The face-centered cubic NPs are created by reacting AgNO<sub>3</sub> with biological solutions, with small differences in peak values depending on the kind of extract, the presence of metabolites, and the binding characteristics [40]. It's noteworthy to note that most scientists [37, 41] who produced plant-derived nanoparticles seem to have attained a similar crystal structure.

#### UV-Visible spectroscopy

UV-Vis spectroscopy is one of the primary techniques for identifying and quantifying the production of NPs. UV-Vis spectroscopy was utilized to confirm the stability of the synthesized AgNPs since the plasmon band of Ag is sensitive to the size and shape of the generated NPs [42].

UV-visible spectroscopy is an important step in confirming the synthesis of Ag-NPs and the color change. When the *Camellia sinensis* extract was mixed with an aqueous solution of AgNO<sub>3</sub>, this resulted in a change of color. This change in color is a result of the collective oscillation of free electron of silver nanoparticles in resonance with the light wave in silver nanoparticle synthesis and this oscillation gives a typical peak value. UV-visible spectra of the plant extracts without AgNO<sub>3</sub> solution and with it were shown in Fig. 5 and 6. The existence of many chemical compounds known to interact with silver ions is indicated by the faint absorption peak at 200 nm. The type, size, and morphologies of the NPs generated the dielectric constant of the medium and temperatures, as well as their interparticle distances, all have a remarkable impact on the surface plasmon resonance absorbance [43, 44]. The

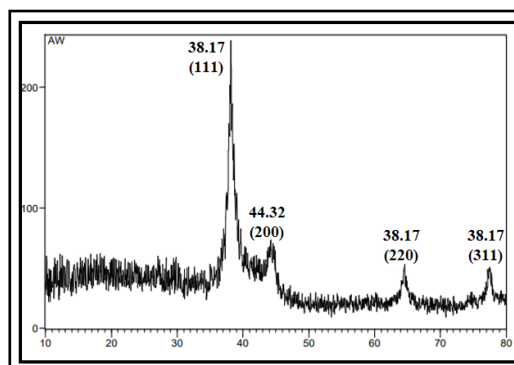


Fig. 3. XRD pattern of CAgNPs methanolic extract.

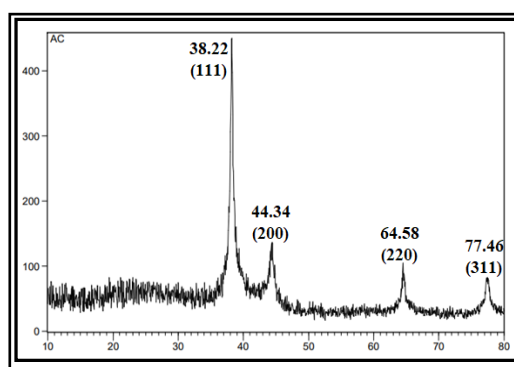
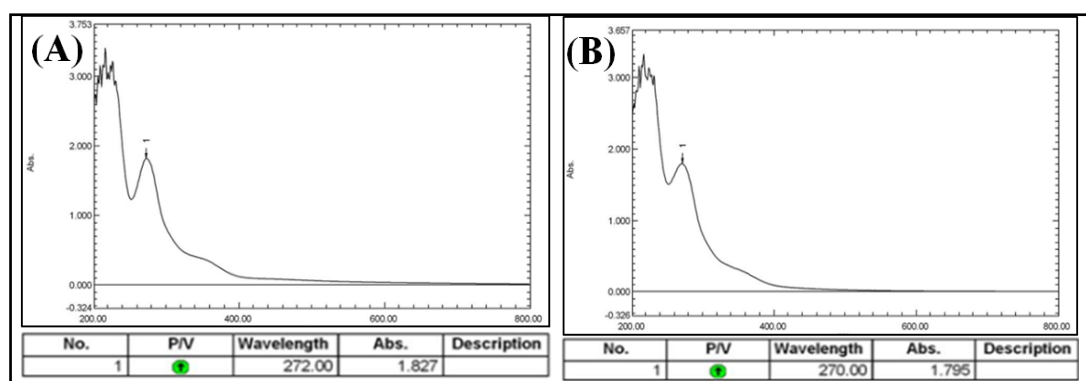
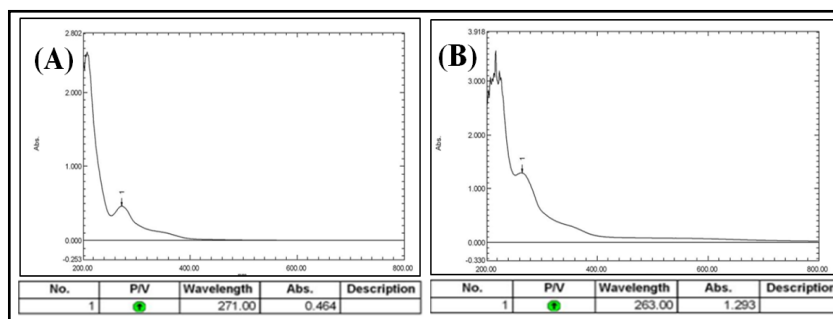


Fig. 4. XRD pattern of CAgNPs aqueous extract.

**Fig. 5.** UV-Visible spectral analysis of (A): *Camellia sinensis* aqueous extract, (B): synthesized (CAgNPs) aqueous extract.



**Fig. 6.** UV-Visible spectral analysis of (A): *Camellia sinensis* methanolic extract, (B): synthesized (CAgNPs) methanolic extract.

absorption spectrum was recorded between 200 nm and 800 nm. It is observed that the silver surface plasmon resonance band centered at 263 nm in the (CAgNPs) aqueous extract and 270 nm in the methanolic (CAgNPs) extract, in comparison with UV Test for *Camellia sinensis* methanolic and aqueous extract (271 and 272) nm respectively.

This result was in line with Bhat et al. [36] findings that silver nanoparticles produced by biosynthesis were virtually spherical, solitary (25–50 nm), or found in clusters (100 nm). Githala et al. [45] measured the size and shape of particles using an atomic force microscope and found that silver particles had an amorphous polygonal shape and sizes ranging from 1.0 to 130 nm. The average size of a nanoparticle was 63.3 nm. Although the diameters of the Ag, ZnO, and LiO<sub>2</sub> particles ranged from 0 to 1.80 nm, 0 to 1.80 nm, and 0 to 2.24 nm, respectively, the Ag and ZnO particles were irregular, but the LiO<sub>2</sub> particles seemed elongated and irregular [46].

#### *Analysis of the zeta potential*

For the aqueous and methanolic extracts of the synthesized compounds, the nanoparticles' zeta potential values were -30.31 and -32.33 mV respectively, as shown in (Fig. 7 and 8).

The zeta analysis plays a significant role in determining the stability of colloidal dispersions. The magnitude of the zeta potential describes the strength of electrostatic attraction between nearby, similarly charged particles in dispersion. Strong zeta potentials provide stability to molecules and particles that are tiny enough, indicating that the solution or dispersion will be resistant to aggregation. Low zeta potentials coagulate or flocculate because the dispersion may fracture and flocculate if attractive forces overcome the repulsion, but high zeta potentials (positive or negative) are electrically stable. The zeta potential of the nanoparticles should typically be greater than +30 mV or lower than -30 mV [47].

Surega [48] showed that the zeta analysis of green-produced AgNPs was -41.7, -27.9, and -37.2 mV using plant extracts *Tridax procumbens*, *Euphorbia hirta*, and *Azadirachta indica*. The very stable nature of AgNPs created using *T. procumbens* extract was revealed

by the wide range of -41.7 mV in the Zeta potential. Using *Vitex negundo* leaf extract, Anandalakshmi and Venugobal [49] created AgNPs with a zeta potential of -13.5mV, indicating incipient instability.

Both the durability of the produced nanoparticles and the decrease in silver ions may be related to a number of the physiologically active compounds present in natural extracts. Phytochemicals such phenolics, coumarins, terpenoids, glycosides, alkaloids, and tannins may serve as bioreductants in this green synthesis method by converting silver ions into Ag-NPs. Additionally, it's probable that the proteins and peptides in *Camellia sinensis* extracts will promote the synthesis of silver nanoparticles and reduce the amount of silver ions in silver [50]. Furthermore, proteins' carbonyl groups can deposit a coating layer on the surface of Ag-NPs because they have a significant affinity for connecting with metal nanoparticles; the resulting nanoparticles are more stable in aquatic settings and less prone to agglomerate [51].

#### High-performance liquid chromatography (HPLC)

Using the HPLC technique, the phenolic content of the different CAgNPs was analyzed. Two phenolic components, gallic acid and caffeine, were found in the (CAgNPs) methanolic and aqueous extracts, (Fig. 9 and 10) respectively, in comparison to standard chemicals (Fig. 11).

When extracting phenols and other active chemicals from plant raw materials many; factors such as preparation time, temperature, and the ratio of dry herbal material to solvent are crucial [52]. Thus, the origin and chemo-type of the plant raw material, the choice of solvent, and the extraction techniques all have a significant impact on the amount of phenolic chemicals present in the extracts. Plant polyphenols are extracted using organic solvents such as methanol, ethanol, ethyl acetate, and others [53].

Understanding the chemical makeup of plants is advantageous for the discovery of therapeutic agents as well as for other reasons, such as the potential for new sources of economically viable plant

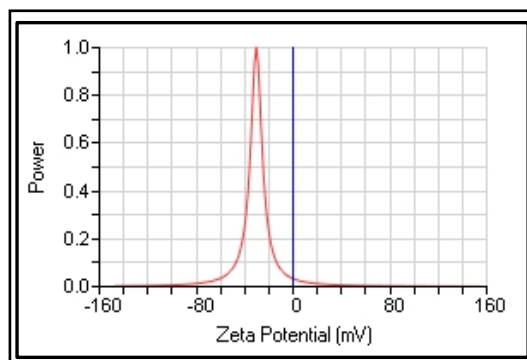


Fig. 7. The zeta potential value of CAgNPs aqueous extract.

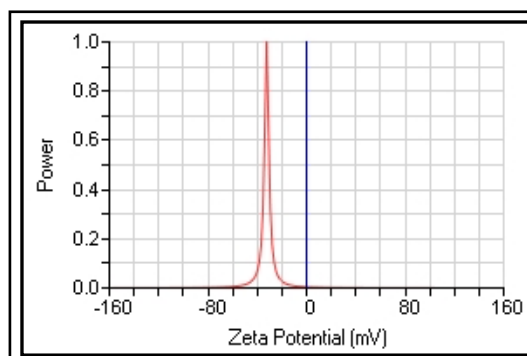


Fig. 8. The zeta potential value of CAgNPs methanolic extract.

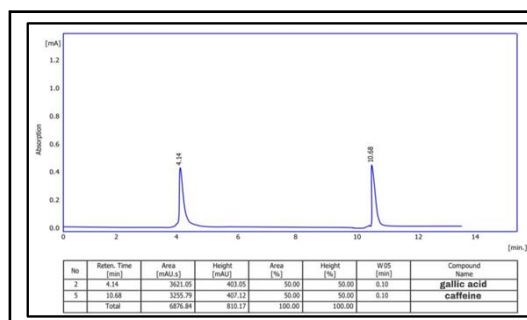


Fig. 9. HPLC chromatogram of phenolic chemicals in methanolic extract of (CAgNPs).

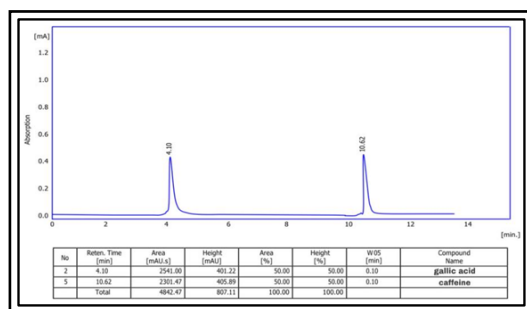
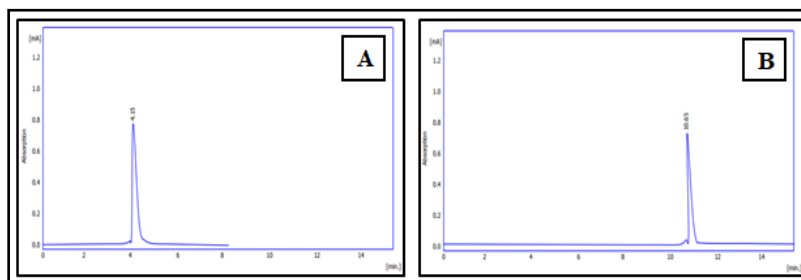


Fig. 10. HPLC chromatogram of phenolic chemicals in aqueous extract of (CAgNPs).

**Fig. 11.** HPLC chromatogram of phenolic chemicals standards (A): gallic acid, (B): caffeine.



compounds for the synthesis of complex chemicals and the potential significance of plant compounds. Treatments and their continued use as medicinal sources that produce biologically active substances are crucial for preserving human health [54]. Phytochemicals, or more specifically, phytoprotectants, are organic, physiologically active substances that are naturally present in plants and function as a defense mechanism against illness [55].

### *Antibacterial activity of (CAgNPs) extracts*

#### *Disk diffusion method.*

The disk-diffusion technique was used to assess the antibacterial activity of (CAgNPs) extracts on *S. aureus* isolates. The results revealed that the methanolic extract of (CAgNPs) was more efficient than the aqueous extract at doses of 375 and 750 mg/ml, giving the greatest inhibition zone values of 15.67 and 20.33 mm respectively in the *S. aureus* isolate No. 9, when compared with the (CAgNPs) aqueous extract which gave inhibition zone 12.33 and 15.67 mm respectively with significant difference ( $P \leq 0.01$ ), as shown in (Table 2).

**Table 2.** Antibacterial activity of silver nanoparticles *Camellia sinensis* extracts (CAgNPs) *S. aureus* isolates. (St): *Staph. Aureus*. The numbers in the table mention to inhibition zone measured in (mm)

No. of Isolate	Methanolic (AgNPs) extract		Aqueous (AgNPs) extract		LSD value
	375 (ppm)	750 (ppm)	375 (ppm)	750 (ppm)	
St <sub>1</sub>	14.33 ± 0.58	19.33 ± 0.58	11.33 ± 0.58	15.33 ± 0.58	1.582**
St <sub>2</sub>	15.33 ± 0.58	18.33 ± 0.58	10.67 ± 0.58	13.33 ± 0.58	1.582**
St <sub>3</sub>	13.33 ± 0.58	17.33 ± 0.58	9.33 ± 0.58	11.33 ± 0.58	1.582**
St <sub>4</sub>	14.33 ± 0.58	18.33 ± 0.58	10.33 ± 0.58	13.33 ± 0.58	1.582**
St <sub>5</sub>	12.33 ± 0.58	16.33 ± 1.16	10.33 ± 0.58	12.33 ± 1.16	2.501**
St <sub>6</sub>	13.33 ± 0.58	18.33 ± 0.58	11.33 ± 0.58	15.33 ± 0.58	1.582**
St <sub>7</sub>	12.33 ± 1.16	16.33 ± 1.16	9.67 ± 0.58	13.33 ± 1.16	2.852**
St <sub>8</sub>	15.33 ± 0.58	18.33 ± 0.58	11.33 ± 0.58	13.67 ± 0.58	1.582**
St <sub>9</sub>	15.67 ± 0.58	20.33 ± 0.58	12.33 ± 0.58	15.67 ± 0.58	1.582**
St <sub>10</sub>	12.33 ± 0.58	18.67 ± 0.58	9.33 ± 0.58	11.33 ± 0.58	1.582**
LSD value	1.529**	1.697**	1.341**	1.697**	----

No. of Isolate	Methanolic (AgNPs) extract		Aqueous (AgNPs) extract		LSD value
	375 (ppm)	750 (ppm)	375 (ppm)	750 (ppm)	
St <sub>1</sub>	14.33 ± 0.58	19.33 ± 0.58	11.33 ± 0.58	15.33 ± 0.58	1.582**
St <sub>2</sub>	15.33 ± 0.58	18.33 ± 0.58	10.67 ± 0.58	13.33 ± 0.58	1.582**
St <sub>3</sub>	13.33 ± 0.58	17.33 ± 0.58	9.33 ± 0.58	11.33 ± 0.58	1.582**
St <sub>4</sub>	14.33 ± 0.58	18.33 ± 0.58	10.33 ± 0.58	13.33 ± 0.58	1.582**
St <sub>5</sub>	12.33 ± 0.58	16.33 ± 1.16	10.33 ± 0.58	12.33 ± 1.16	2.501**
St <sub>6</sub>	13.33 ± 0.58	18.33 ± 0.58	11.33 ± 0.58	15.33 ± 0.58	1.582**
St <sub>7</sub>	12.33 ± 1.16	16.33 ± 1.16	9.67 ± 0.58	13.33 ± 1.16	2.852**
St <sub>8</sub>	15.33 ± 0.58	18.33 ± 0.58	11.33 ± 0.58	13.67 ± 0.58	1.582**
St <sub>9</sub>	15.67 ± 0.58	20.33 ± 0.58	12.33 ± 0.58	15.67 ± 0.58	1.582**
St <sub>10</sub>	12.33 ± 0.58	18.67 ± 0.58	9.33 ± 0.58	11.33 ± 0.58	1.582**
LSD value	1.529**	1.697**	1.341**	1.697**	----

According to this study, the antibacterial activity appears to be linked to the high concentration of phenolic chemicals (such as caffeine and gallic acid) found in the methanolic and aqueous extracts of CAgNPs. Numerous phenolic compounds have antibacterial properties against plant diseases that can also be used to combat infections that affect humans. Additionally, many derived phenolic compounds' antibacterial activity employ pathways distinct from those of traditional medicines, which suggest they may be useful in advancing antibacterial therapy [56].

The antibacterial activity of the CAgNPs extracts against isolated *S. aureus* was quite strong. Due to their size, they are able to quickly access bacteria's nuclei and exhibit a sizable and outstanding surface area, which is where interaction with bacteria is most intense. The AgNPs antibacterial activity methods vary depending on their size, shape, surface, surface charge, solubility, exposure period, and concentration [57]. The inactivation of cellular proteins, DNA damage, and enzyme degradation are a few of the several hypothesised reasons for AgNPs' beneficial antibacterial action [58].

Because of their smaller size, AgNPs are likely to have adhered to the bacterial cell membrane's surface and disrupted vital processes like permeability and respiration. They may then have easily entered the bacteria's interior and caused additional harm, possibly by interacting with sulphur- and phosphorus-containing substances like DNA to cause cell lysis. Additionally, the majority of recent studies have identified the following mechanisms of action for nanocomposites: adhesion to microbial cells, physical contact-induced cell wall lysis, and ROS production, particle penetration into the cell, oxidative stress-induced protein and DNA damage, and facilitation of internalization. In addition to size, different formulations with various particle shapes and surface charges may also have an impact on the inherent characteristics of the NPs and maybe have an impact on their antibacterial activity [59]. Almalah et al [60]., claimed that silver nanoparticles are effective at inhibiting both gram-positive and gram-negative bacteria when compared to green synthesis of AgNPs, giving a zone of inhibition of 25 mm against *S. aureus*, 24 mm against *K. pneumonia*, and 22 mm against *P. aeruginosa* and *A. baumannii*. Additionally, Ansari and Alzohairy [61] and Ahmed et al [62]., noted that the antibacterial activity increased with the rising Ag-NP concentrations. According to Huq [63], Ag-NPs have antibacterial activity against *S. aureus*, *P. aeruginosa*, and *E. coli* with inhibition zones 16.1, 16.6, and 13.4 mm, respectively.

### Measurement the (MIC) of the CAgNPs extracts

The CAgNPs MIC was determined in broth microdilution method using a 96-well microtiter plate. Resazurin's color, a sign of bacterial growth, was used to calculate the lowest inhibitory concentration.

The MIC result demonstrated that the methanolic extract of CAgNPs was superior to the aqueous extract. The CAgNPs methanolic extract's MIC were 23.43 µg/ml for isolates No.1, 2, 5 and 6, while the isolates No. 4 and 8 was 11.718 µg/ml. the MIC results of the aqueous CAgNPs extract on all *S. aureus* isolates were 46.87 µg/ml except isolates No. 3 and 6 which were 11.718 and 93.75 µg/ml respectively, as shown in (Table 3) and (Fig. 12 and 13).

According to the study's findings, methanolic extract of the *Camellia sinensis* contained nanoparticles with a better biological effectiveness against *S. aureus* than aqueous extract. This is because the methanolic extract might contain more quantitative and qualitative phenolic compounds than the CAgNPs aqueous extract, and

**Table 3.** MIC of *Camellia sinensis* silver nanoparticles (CAgNPs) methanolic and aqueous leaves extracts on *S. aureus* isolates. Staph. Aureus

Isolate	Silver nanoparticles	Silver nanoparticles
	aqueous extract (µg/ml)	methanolic extract (µg/ml)
	MIC (µg/ml)	MIC (µg/ml)
St <sub>1</sub>	46.87	23.43
St <sub>2</sub>	46.87	23.43
St <sub>3</sub>	11.718	46.87
St <sub>4</sub>	46.87	11.718
St <sub>5</sub>	46.87	23.43
St <sub>6</sub>	93.75	23.43
St <sub>7</sub>	46.87	46.87
St <sub>8</sub>	46.87	11.718
St <sub>9</sub>	46.87	46.87
St <sub>10</sub>	46.87	46.87

these phytochemicals can help with a variety of antimicrobial activities. The plant chemicals that are included in the plant extracts play the job of reducing and stabilizing agents.

According to Al-Aboudi and AL-Azawi [64], flavonoids compounds have been discovered to be powerful antibacterial agents against a variety of pathogenic microorganisms *in vitro*. Furthermore, it has been said that nanoparticle sizes have a substantial impact on how successful they are in killing bacteria [65]. Because of their large surface areas, charges, adsorption, and chemical reactivity, the many forms of this nanoscale size can interact with biological systems in a way that severely inhibits them [66]. Therefore, the CAgNPs nanoscale diameters were crucial to their effectiveness against bacteria. The outcomes of this study agree with those of Abdul elah Mohammad and Al-Jubouri [67], who found that the nanoparticles displayed potent antibacterial activity against both Gram positive and negative bacteria.

#### Anti-Biofilm Activity of CAgNPs extracts

A biofilm is a densely packed community of microorganisms that grows on both living and nonliving surfaces and envelops itself in secreted polymers. Biofilm-associated disorders are typically difficult to treat due to multidrug resistance [68], hence it is essential to discover new chemicals that are effective in preventing bacterial biofilm development.

The anti-biofilm in *S. aureus* was increased when CAgNPs methanolic extract were used compared with the CAgNPs aqueous extract, the CAgNPs methanolic extract inhibited 80, 90, and 100 percent of *S. aureus* biofilm formation in 23.43, 46.87 and 93.75 µg/ml respectively, as shown in (Table 4), while the anti-biofilm activity of the CAgNPs aqueous extract on *S. aureus* isolates was 80% and 100% of the biofilm formation in 46.87 and 93.75 µg/ml respectively, as shown in table (Table 5).

Biofilm development has been linked to antibiotic resistance in bacterial populations [69]. The concentration-dependent inhibition or reduction of biofilm development served as evidence for the anti-biofilm effect of the phenolic compounds. Flavonoids may encourage

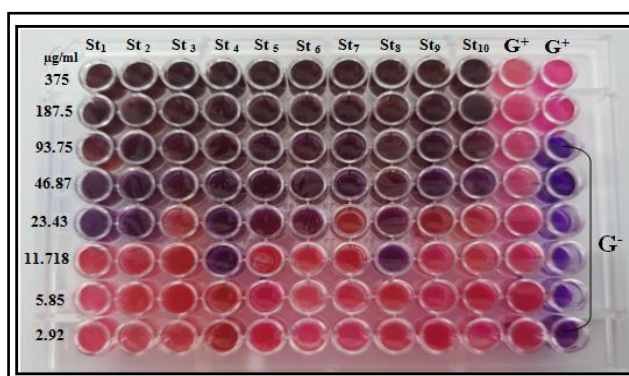


Fig. 12. MIC of methanolic CAgNPs extract on *S. aureus* isolates.

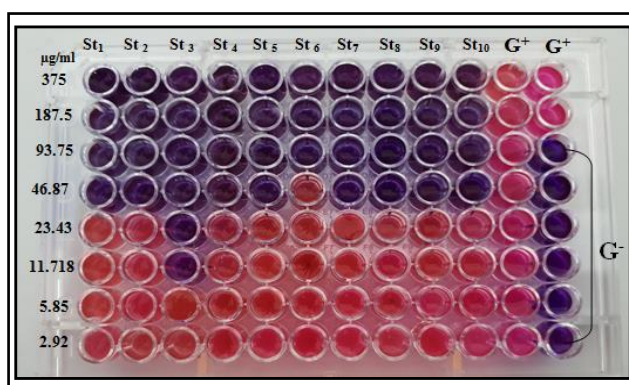


Fig. 13. MIC of aqueous CAgNPs extract on *S. aureus* isolates.

Table 4. Biofilm development of *S. aureus* isolates before and after treatment with methanolic extract of CAgNPs St: *Staphylococcus aureus*, control negative (cut off) = 0.2

No of isolates	Before treatment	After treatment with silver nanoparticles methanolic extract (µg/ml)							
		2.92	5.85	11.718	23.43	46.87	93.75	187.5	375
St <sub>1</sub>	Strong	Weak	No Biofilm						
St <sub>2</sub>	Strong	Weak	Weak	Weak	Biofilm	Biofilm	Biofilm	Biofilm	Biofilm
St <sub>3</sub>	Strong	Weak	Weak	Biofilm	Biofilm	Biofilm	Biofilm	Biofilm	Biofilm
St <sub>4</sub>	Strong	Weak	Weak	Weak	Weak	Weak	Biofilm	Biofilm	Biofilm
St <sub>5</sub>	Strong	Weak	Weak	Weak	Biofilm	Biofilm	Biofilm	Biofilm	Biofilm
St <sub>6</sub>	Strong	Weak	Weak	Biofilm	Biofilm	Biofilm	Biofilm	Biofilm	Biofilm
St <sub>7</sub>	Strong	Weak	Weak	Weak	Biofilm	Biofilm	Biofilm	Biofilm	Biofilm
St <sub>8</sub>	Strong	Moderate	Weak	No Biofilm					
St <sub>9</sub>	Strong	Moderate	Weak	Weak	No Biofilm				
St <sub>10</sub>	Strong	Moderate	Weak	Weak	Biofilm	Biofilm	Biofilm	Biofilm	Biofilm

bacterial aggregation by partly lysing bacteria. Therefore, membrane fusion restricts the active absorption of nutrients across a smaller membrane area [70].

The antibacterial activity of phenols has been attributed to a variety of processes, including interactions with bacterial proteins and cell walls, cytoplasmic membrane degradation, reduced fluidity of membranes, and suppression of energy metabolism, nucleic acid synthesis, and cell wall and cell formation [71, 72].

Liu et al [73]. showed that gallic acid penetrated the biofilm and killed *S. aureus*. Furthermore, it is possible to hypothesize that the presence of plant extracts in growth medium caused an unfavorable situation that may prevent cell attachment or decrease surface adhesion, AgNPs green production significantly affects the development of bacterial biofilms as well [74]

## Conclusion

According to the findings of the present study, it can be said that the methanolic and aqueous leaves extracts from *Camellia sinensis* are a successful method for producing CAgNPs. The synthesized CAgNPs also have significant antibacterial activity against *S. aureus* and, depending on the concentrations, as well as, inhibit *S. aureus* biofilm formation.

## Acknowledgements

We hereby confirm that all the Figures and Tables in the manuscript are mining ours. Besides, the Figures and images, which are not mine ours, have been given the permission for re-publication attached with the manuscript.

### Ethical Clearance

The project was approved by the local ethical committee in University of Baghdad.

## Disclosure Statement

The authors have nothing to disclose.

## References

- 1 De Gregorio E, Esposito A, Vollaro A, De Fenza M, D'Alonzo D, Migliaccio A. and Guaragna, A. N-Nonyloxypropyl-1-Deoxynojirimycin inhibits growth, biofilm formation and virulence factors expression of *Staphylococcus aureus*. *Antibiotics* 2020;9:362.
- 2 Khan SA, Shahid S, Lee C-SS. Green synthesis of gold and silver nanoparticles using leaf extract of *Clerodendrum inerme*; characterization, antimicrobial, and antioxidant activities. *Biomol. Ther* 2020;10:835.

**Table 5.** Biofilm development of *S. aureus* isolates before and after treatment with aqueous extract of CAgNPs St: *Staphylococcus aureus*, control negative (cut off) = 0.2

No of isolates	Before treatment	After treatment with silver nanoparticles aqueous extract (µg/ml)							
		2.92	5.85	11.718	23.43	46.87	93.75	187.5	375
St <sub>1</sub>	Strong	Moderate	Moderate	No Biofilm					
St <sub>2</sub>	Strong	Strong	Moderate	Moderate	Moderate	No Biofilm	No Biofilm	No Biofilm	No Biofilm
St <sub>3</sub>	Strong	Weak	Weak	Weak	Weak	No Biofilm	No Biofilm	No Biofilm	No Biofilm
St <sub>4</sub>	Strong	Weak	Weak	Weak	Weak	No Biofilm	No Biofilm	No Biofilm	No Biofilm
St <sub>5</sub>	Strong	Moderate	Weak	Weak	Weak	No Biofilm	No Biofilm	No Biofilm	No Biofilm
St <sub>6</sub>	Strong	Weak	Weak	Weak	Weak	No Biofilm	No Biofilm	No Biofilm	No Biofilm
St <sub>7</sub>	Strong	Moderate	Weak	Weak	Weak	Weak	Weak	No Biofilm	No Biofilm
St <sub>8</sub>	Strong	Moderate	Weak	Weak	Weak	Weak	Weak	No Biofilm	No Biofilm
St <sub>9</sub>	Strong	Moderate	Weak	Weak	Weak	No Biofilm	No Biofilm	No Biofilm	No Biofilm
St <sub>10</sub>	Strong	Moderate	Weak	Weak	Weak	No Biofilm	No Biofilm	No Biofilm	No Biofilm

- 3 Khan SA, Shahid S, Mahmood T, Lee C.-S. Contact lenses coated with hybrid multifunctional ternary nanocoatings (Phytomolecule-coated ZnO nanoparticles:Gallic acid:tobramycin) for the treatment of bacterial and fungal keratitis. *Acta Biomater* 2021;128:262–276.
- 4 Khan SA, Lee CS. Recent progress and strategies to develop antimicrobial contact lenses and lens cases for different types of microbial keratitis. *Acta Biomater* 2020;113,101–118.
- 5 Yasin SA, AL-Azawi AH. Antibacterial Activity of Conocarpus Erectus Leaves Extracts on Some Microorganisms Isolated From Patients With Burn Infection. *Plant Archives* 2019;19:583-589.
- 6 Qurat -Ul-Ain, Raja A-Q, Sarfraz A. Mechanism of Action of bio-inspired nanosilver particles. *Bioinspired, Biomimetic and Nanobiomaterials* 2020;7:174-186.
- 7 World Health Organization (WHO). *Basic laboratory procedures in clinical bacteriology*. 2<sup>nd</sup> ed. Genev, Switzerland 2003.
- 8 Clinical Laboratory Standards Institute (CLSI-M100). Performance standards for antimicrobial susceptibility testing, 31st edition, CLSI document m100. Retrieved Jan 06, 2023 from [https://clsi.org/media/z2uhcbmv/m100ed31\\_sample.pdf](https://clsi.org/media/z2uhcbmv/m100ed31_sample.pdf).
- 9 Patel FM, Goswami PN, Khara R. Detection of Biofilm formation in device associated clinical bacterial isolates in cancer patients. *Sri Lankan Journal of Infectious Diseases* 2016;6:43-50.
- 10 Kirmusaoglu S. The Methods for Detection of Biofilm and Screening Antibiofilm Activity of Agents. In *Exopolysaccharides Methods of Preparation and Application*. In *technology Open* 2019;1-DOI:<http://dx.doi.org/10.5772/intechopen.84411>.
- 11 Ansari P, Azam S, Seidel, V, Abdel-Wahab YH. In vitro and in vivo antihyperglycemic activity of the ethanol extract of Heritiera fomes bark and characterization of pharmacologically active phytomolecules. *Journal of Pharmacy and Pharmacology* 2022;74:415-425
- 12 Krishnadhass L, Santhi R, Annapurani S. Green Synthesis of Silver Nanoparticles from the Leaf Extract of *Volkameria inermis*. *International Journal of Pharmaceutical and Clinical Research*, 2017;9:610-616.
- 13 Hammodi HF, Rashid IH, Oraibi AG. "Green biosynthesis, Identification and characterization of Ag and Zn nanoparticles using Ivy (*Epipremnum aureum*) plant extract," *Plant Arch* 2019;19:959–965.
- 14 Ojha S, Sett A, Bora U. Green synthesis of silver nanoparticles by *Ricinus communis* var. *carmencita* leaf extract and its antibacterial study. *Advances in Natural Sciences: Nanoscience and Nanotechnology* 2017 8:35-39.
- 15 Anandalakshmi K, Venugobal J, Ramasamy V. Characterization of silver nanoparticles by green synthesis method using *Pedaliium murex* leaf extract and their antibacterial activity. *Appl Nanosci* 2016;6:399-408.
- 16 Lakshmanan G, Kalaiichelvan SA, Murugesan K. Plant-mediated synthesis of silver nanoparticles using fruit extract of *Cleome viscosa* L.: Assessment of their antibacterial and anticancer activity 2018;4:61-68.
- 17 Elbossaty WF. Green tea as biological system for the synthesis of silver nanoparticles. *J biotechnol biomater* 2017; 7:2.
- 18 Aljabali AAA, Akkam Y, Al-Zoubi MS, Al-Batayneh KM, AlTrad B, Abo Alrob O, Alkilany AM, Benamara M, Evans DJ. Synthesis of Gold Nanoparticles Using Leaf Extract of *Ziziphus zizyphus* and their Antimicrobial Activity. *Nanomaterials J* 2018;8:174-188.
- 19 Mizzi L, Chatzitzika C, Gatt R, Valdramidis V. HPLC analysis of phenolic compounds and flavonoids with overlapping peaks. *Food technology and biotechnology* 2020;58,12-19.
- 20 Razmavar S, Mahmood AA, Salmah BI, Pouya H. Antibacterial Activity of Leaf Extracts of *Baeckea frutescens* against Methicillin-Resistant *Staphylococcus aureus*. *BioMedical Research International* 2014;2014:521287.
- 21 Ohikhena FU, Wintola OA, Afolayan AJ. Evaluation of the Antibacterial and Antifungal Properties of *Phragmanthera capitata* (Sprengel) Balle (Loranthaceae), a Mistletoe Growing on Rubber Tree, Using the Dilution Techniques. *Scientific World Journal* 2017;2017:9658598.
- 22 Sadari H, Owlia P. Detection of multidrug resistant (MDR) and extremely drug resistant (XDR) *P. aeruginosa* isolated from patients in Tehran, Iran. *Iranian Journal of Pathology* 2015;10:265.
- 23 Yayan J, Ghebremedicalhin B, Rasche K. Antibiotic resistance of *Pseudomonas aeruginosa* in pneumonia at a single university hospital center in Germany over a 10-year period. *Plos One* 2015;10:1-20.
- 24 Djeussi DE, Noumedicalem JAK, Seukep JA. Antibacterial activities of selected edible plants extracts against multidrug-resistant gram-negative bacteria. *BMC Complementary and Alternative Medicine* 2013;13:164.
- 25 AbdulRazzaq AB, AbdulMuhsin MS, Kais KG. Detection of *vanA* and *vanB* genes Among Vancomycin Resistant *Staphylococcus aureus* Isolated from Clinical Samples in Baghdad Hospitals, *Iraqi Journal of Biotechnology* 2022;20:19-25.

- 26 Jabur EQ, Kandala N. The Production of Biofilm from Methicillin Resistant Staphylococcus aureus Isolated from Post-Surgical Operation Inflammation, Iraqi Journal of Science 2022;63:3688-3702.
- 27 Al-Nuaimi RS, Garjes SG, Mahmood MB. Isolate Bacterial Contamination from Iraqi Currencies Notes and Determination of Their Resistance to Antibiotic, Ann Coll Med Mosul 2022;44:171-180.
- 28 Bronowskil C, James CE, Winstanley C. Role of environmental survival in transmission of campylobacter jejuni. FEMS Microbiol Lett 2014;356:8-19.
- 29 Ramos G, Rocha J, Tuon F. Seasonal humidity may influence Pseudomonas aeruginosa hospital acquired infection rates. International. J Infect Dis 2013;17:757-761.
- 30 Khudhur IM. Investigating the ability of some bacterial species to produce slime Layer. Raf J Sci 2013;24:36-49.
- 31 Bhadra MP, Sreedhar B, Patra CR. Potential theranostics application of bio-synthesized silver nanoparticles (4-in-1 system). Theranostics 2014;4:316-335.
- 32 Salleh A, Naomi R, Utami ND, Mohammad AW, Mahmoudi E, Mustafa N. The potential of silver nanoparticles for antiviral and antibacterial applications: A mechanism of action. J Nanomater 2020;10:20.
- 33 Al-Khafaji AR, Al-Azawi AH. Green Method Synthesis of Silver Nanoparticles Using Leaves Extracts of Rosmarinus officinalis. Iraqi journal of biotechnology 2022;21:251-267.
- 34 Saliem AH, Ibrahim OM, Salih SI. Biosynthesis of Silver Nanoparticles using Cinnamon zeylanicum Plants Bark Extract. Kufa Journal For Veterinary Medical Sciences 2016;7:51-63.
- 35 Kouvaris P, Delimitis A, Zaspalis V, Papadopoulos D, Tsipas SA, Michailidis N. (). Green synthesis and characterization of silver nanoparticles produced using Arbutus Unedo leaf extract. Materials Lett 2012;76:18-20.
- 36 Shareef AA, Hassan ZA, Kadhim MA, Al-Mussawi AA. Antibacterial Activity of Silver Nanoparticles Synthesized by Aqueous Extract of Carthamus oxycantha M. Bieb. Against Antibiotics Resistant Bacteria. Baghdad Science Journal 2022;19:0460-0460.
- 37 Salari S, Bahabadi SE, Samzadeh-Kermani A, Yosefzaei F. In-vitro evaluation of antioxidant and antibacterial potential of green synthesized silver nanoparticles using Prosopisfarcta fruit extract. Iranian Journal of Pharmaceutical Research 2019;18:430-445.
- 38 Ssekatawa K, Byarugaba D, Kato C, Nakavuma J, Wampande E, Ejobi F, Nxumalo E. Physiochemical properties and antibacterial activity of silver nanoparticles green synthesized by Camellia sinensis and Prunus africana extracts. Research square. 2021; | January 21; DOI: <https://doi.org/10.21203/rs.3.rs-143995/v1>.
- 39 Rakaa JM, Obaid AS. Preparation of Nanoparticles in an Eco-friendly Method using Thyme Leaf Extracts. Baghdad Science Journal 2020;17.
- 40 Salih HH. Biosynthesis of Silver Nanoparticles by Using Green tea (Camellia sinensis) Extracts. Baghdad Science Journal 2024;21:1470-1482.
- 41 Waris M, Nasir S, Rasule A, Yousaf I. Evaluation of larvicidal efficacy of Ricinus communis (Castor) plant extract and synthesized green silver nanoparticles against Aedes albopictus. J Arthropod-Borne Dis 2020; 14:162-172.
- 42 Asimuddin M, Shaik MR, Adil SF, Siddiqui MRH, Alwarthan A, Jamil K, Khan M. Azadirachta indica based biosynthesis of silver nanoparticles and evaluation of their antibacterial and cytotoxic effects. J King Saud Univ Sci 2020;32:648-656.
- 43 Venugopal K, Rather HA, Rajagopal K, Shanthi MP, Sheriff K, Illiyas M, Maaza M. Synthesis of silver nanoparticles (Ag NPs) for anticancer activities (MCF 7 breast and A549 lung cell lines) of the crude extract of Syzygium aromaticum. J. Photochem. Photobiol B Biol 2017;167:282-289
- 44 Mohammad DAE, Al-Jubouri SHK. Comparative antimicrobial activity of silver nanoparticles synthesized by Corynebacterium glutamicum and plant extracts. Baghdad Sci J 2019;16:689-696.
- 45 Githala CK, Raj S, Dhaka A, Mali, SC. Trivedi R. Phyto-fabrication of silver nanoparticles and their catalytic dye degradation and antifungal efficacy. Front Chem 2022;10.
- 46 González-Ballesteros N, Prado-López S, Rodríguez-González JB, Lastra M, Rodríguez-Argüelles MC. Green synthesis of gold nanoparticles using brown algae Cystoseira baccata: Its activity in colon cancer cells. Colloids and Surfaces B: Biointerfaces 2017;153:190-198.
- 47 Elamawi RM, Al-Harbi RE, Hendi AA. Biosynthesis and characterization of silver nanoparticles using Trichoderma longibrachiatum and their effect on phytopathogenic fungi. Egypt J Biol Pest Control 2018;28:1-11.

- 48 Surega R. Green synthesis of bioactive silver nanoparticles using plant extracts and their antinemic properties. PhD. Thesis, College of Agriculture, Tamil Nadu Agricultural University, Coimbatore. 2015.
- 49 Anandalakshmi K, Venugobal J. Green synthesis and characterization of silver nanoparticles using Vitex negundo (Karu Nochchi) Leaf Extract and its Antibacterial Activity. *Med Chem (Los Angeles)* 2017;7: 218-225.
- 50 Dhand V, Soumya L, Bharadwaj S, Chakra S, Bhatt D, Sreedhar B. Green synthesis of silver nanoparticles using Coffea arabica seed extract and its antibacterial activity. *Mater.Sci Eng C* 2016;58:36-43.
- 51 Nikam SA, Chaudhari SP. Biosynthesis of Silver Nanoparticles from Polyphenolic Extract of *Baliospermum solanifolium* using Central Composite Design. *Pharm. Res* 2022;14:405-411. DOI: 10.5530/pres.14.4.59.
- 52 Shanaida M, Kernychna I, Shanaida YU. Chromatographic analysis of organic acids, amino acids, and sugars in *Ocimum americanum* L. *Acta Poloniae Pharmaceutica – Drug Research* 2017;74:729-732.
- 53 Vlase L, Benedec D, Hanganu D, Damian G, Csillag I, Sevastre B. et al. Evaluation of antioxidant and antimicrobial activities and phenolic profile for *Hyssopus officinalis*, *Ocimum basilicum* and *Teucrium chamaedrys*. *Molecules* 2014;19:5490-5507.
- 54 Hameed IH, Al-Rubaye AF, Kadhim MJ. Urinary Tract Infections: Characterization and Herbal Antimicrobial Activity: A Review. *International Journal of Current Pharmaceutical Review and Research* 2017;8,184-191.
- 55 Subashini R, Manoharan A. Phytochemical analysis of the Siddha poly herbal formulation Jaathipalathi Chooranam. *Journal of Research in Biomedical Sciences* 2019;1:71-76.
- 56 Sanver D, Murray BS, Sadeghpour A, Rappolt M, Nelson AL. Experimental modeling of flavonoid bio-membrane interactions. *Langmuir* 2016;32:13234–13243.
- 57 Espinosa JCM, Cerritos RC, Morales MA, Guerrero KP, Contreras RA, Crystals JM. Characterization of silver nanoparticles obtained by a green route and their evaluation in the bacterium of *Pseudomonas aeruginosa*. *Crystals* 2020;10:13.
- 58 Guzman M., Dille J, Godet S. Synthesis and antibacterial activity of silver nanoparticles against gram-positive and gram-negative bacteria. *Nanomedicine: Nanotechnology, Biology and Medicine* 2012;8:37-45.
- 59 Basavegowda N, Baek KH. Multimetallic Nanoparticles as Alternative Antimicrobial Agents: Challenges and Perspectives. *Molecules* 2021;26:912.
- 60 Almalah HI, Alzahrani HA, Abdelkader HS. Green Synthesis of Silver Nanoparticles using *Cinnamomum Zylanicum* and their Synergistic Effect against Multi-Drug Resistance Bacteria. *Journal of Nanotechnology Research* 2019;1:95-107.
- 61 Ansari MA, Alzohairy MA. One-pot facile green synthesis of silver nanoparticles using seed extract of *Phoenix dactylifera* and their bactericidal potential against MRSA. *Evidence-Based Complementary and Alternative Medicine* 2018; doi: 10.1155/2018/1860280.
- 62 Ahmed BA, Saleem MH, Matty FS. Synthesis and Study of the Antimicrobial Activity of Modified Polyvinyl Alcohol Films Incorporated with Silver Nanoparticles. *Baghdad Science Journal* 2023;20:1643-1653.
- 63 Huq M. Green synthesis of silver nanoparticles using *Pseudoduganella eburnea* MAHUQ-39 and their antimicrobial mechanisms investigation against drug resistant human pathogens. *International journal of molecular sciences* 2020;21:1510.
- 64 Al-Aboudi Z. F. and AL-Azawi, A. H: Antibacterial and Antibiofilm Activity of Phenolic Compounds Extracted From *Camellia Sinensis* And Evaluate The Effect On The Gene Expression (Clfa) In *Staphylococcus Aureus*. *Pakistan Journal of Life and Social Sciences* 2024;22:2288-2304.
- 65 Dakal TC, Kumar A, Majumdar RS, Yadav V: Mechanistic basis of antimicrobial actions of silver nanoparticles, *Front Microbiol* 2016;5:2831.
- 66 Wang L, Hu C, Shao L. The antimicrobial activity of nanoparticles: present situation and prospects for the future. *International journal of nanomedicine* 2017;12:1227.
- 67 Abdul elah Mohammad D, Al-Jubouri SH. Comparative antimicrobial activity of silver nanoparticles synthesized by *Corynebacterium glutamicum* and plant extracts. *Baghdad Science Journal* 2019;16;DOI: [http://dx.doi.org/10.21123/bsj.2019.16.3\(Suppl.\)0689](http://dx.doi.org/10.21123/bsj.2019.16.3(Suppl.)0689).
- 68 Kumar L, Chhibber S, Harjai K. Zinger one inhibits biofilm formation and improve Antibiofilm efficacy of ciprofloxacin against *Pseudomonas aeruginosa* PAO1. *Fitoterapia* 2013;90:73–78.
- 69 Rajkumari J, Busi S, Vasu AC, Reddy P. Facile green synthesis of baicalein fabricated gold nanoparticles and their antibiofilm activity against *Pseudomonas aeruginosa* PAO1. *Microbial pathogenesis* 2017;107:261-269.

- 70 Awolola GV, Koorbanally NA, Chenia H, Shode FO, Baijnath H. Antibacterial and anti-biofilm activity of flavonoids and triterpenes isolated from the extracts of *Ficus Sansibarica* warb. Subsp. *Sansibarica* (Moraceae) extracts. *African Journal of Traditional, Complementary Alternative Medicines* 2014;11:124-131.
- 71 Gyawali R, Ibrahim SA. Natural products as antimicrobial agents. *Food control* 2014;46:412-429.
- 72 F. M. Laith and A. H. AL-Azawi. Antibiofilm Activity of *Conocarpus erectus* Leaves Extract and Assessment Its Effect on *pelA* and *algD* Genes on Multi-drug Resistant *Pseudomonas aeruginosa*. *The Egyptian Journal of Hospital Medicine* 2022;89:6961-6969.
- 73 Liu M, Wu X, Li J, Liu L, Zhang R, Shao D, Du X. The specific anti-biofilm effect of gallic acid on *Staphylococcus aureus* by regulating the expression of the *ica* operon. *Food Control*, 2017;73:613-618.
- 74 Shakerimoghaddam A, Razavi D, Rahvar F, Khurshid M, Ostadkelayeh SM, Esmaili SA, et al. Evaluate the effect of zinc oxide and silver nanoparticles on biofilm and *icaA* gene expression in methicillin-resistant *Staphylococcus aureus* isolated from burn wound infection. *Journal of Burn Care and Research*, 2020;41:1253-1259